Transient Evolution of Surface Roughness on Patterned GaAs(001) during Homoepitaxial Growth

H.-C. Kan, S. Shah, T. Tadyyon-Eslami, and R. J. Phaneuf

Department of Physics and Department of Materials Science and Engineering, University of Maryland, and Laboratory for Physical Sciences, College Park, Maryland 20740

(Received 26 September 2003; published 8 April 2004)

We have investigated the length scale dependence of the transient evolution of surface roughness during homoepitaxial growth on GaAs(100), patterning the surface lithographically with an array of cylindrical pits of systematically varied sizes and spacings. Our atomic force microscopy measurements show that the amplitude of the surface corrugation has nonmonotonic behavior in both the length scale dependence and time evolution. This behavior allows us to rule out a number of existing continuum models of growth.

DOI: 10.1103/PhysRevLett.92.146101 PACS numbers: 81.15.Hi, 68.35.Ct, 68.55.Ac, 81.15.Aa

The evolution of the surface roughness during epitaxial growth remains a subject of great interest. Technologically, minimizing interface roughness and thus electron or photon scattering is a crucial concern in electronic and optoelectronic device fabrication. From a scientific point of view, it is an intriguing challenge to construct a model that can describe the essential kinetic and equilibrium surface processes and their mutual interactions to correctly predict the evolution of the surface roughness. To date, most theoretical models [1–7] have attempted to describe the asymptotic behavior of the evolution of surface roughness during epitaxial growth. In practice, however, grown film thicknesses are usually small compared to what would be required to reach the asymptotic limit. Thus, it is the transient response of the surface roughness to growth that is most relevant to describing device fabrication.

Here we report a systematic experimental study of the transient evolution of the surface roughness during growth and its length scale dependence. It has been reported that the initial morphology has a profound effect in the evolution of the surface morphology during growth [8]. Thus, the initial surface morphology becomes a crucial part of the control of the experiment. A nominally ''flat'' surface as typically prepared generally contains poorly controlled and characterized roughness resulting from surface preparation procedures, such as polishing and oxide removal. This poses a major difficulty for both reproducibility and navigation to the same location for repeated measurements. To circumvent this problem, we ''control'' the initial surface morphology by introducing an artificially produced periodic corrugation, with a range of well defined characteristic lateral periods, whose amplitude is significantly larger than that of the roughness resulting from surface preparation. Following the evolution of the pattern amplitude during growth allows us to characterize the lateral length scale dependence of the transient evolution of the surface roughness.

Our experiments were carried out on a GaAs (001) surface, patterned lithographically with an array of cylindrical pits, whose diameter and center-to-center spacing was varied from slightly submicron to over 10 μm in a systematic manner [9]. The initial depth of each pit is approximately 50 nm, more than an order of magnitude larger than the rms roughness resulting from sample preparation processes. Subsequent to patterning, the sample was cycled between a molecular beam epitaxy (MBE) system for homoepitaxial growth and an atomic force microscope (AFM) for measurement of the surface topography. The patterned structure served as an excellent means of navigation that allows us to repeatedly characterize the surface morphology at the same locations after additional growth. In the MBE chamber, the surface oxide was thermally desorbed at a substrate temperature of 640 °C under an arsenic overpressure, followed by GaAs epitaxial growth at a rate of $\sim$2.7 Å/sec with the substrate temperature held at 585 °C. The ratio of the beam equivalent pressure between the As_2 flux and that of the Ga flux during growth was 10:1. After growth of a series of film thicknesses, the sample was removed from the MBE chamber and imaged with tapping mode AFM in air. AFM images from the regions between pits showed that the growth was mostly by island nucleation. In this Letter, we discuss results from regions of the surface on which the center-to-center distance between neighboring pits is twice the initial pit diameter.

Figures 1(a)–1(d) show AFM images of the surface resulting from growth of 500 nm of GaAs onto regions which have been patterned at a series of increasing length scales. All of the images are presented with the same gray scale. The strong contrast between the images shows visibly the length scale dependence of the evolution of the corrugations. The amplitude of the smallest diameter pit array is greatly reduced, and by this point successive corrugations are smeared out along the [$\underline{1}$10] direction.

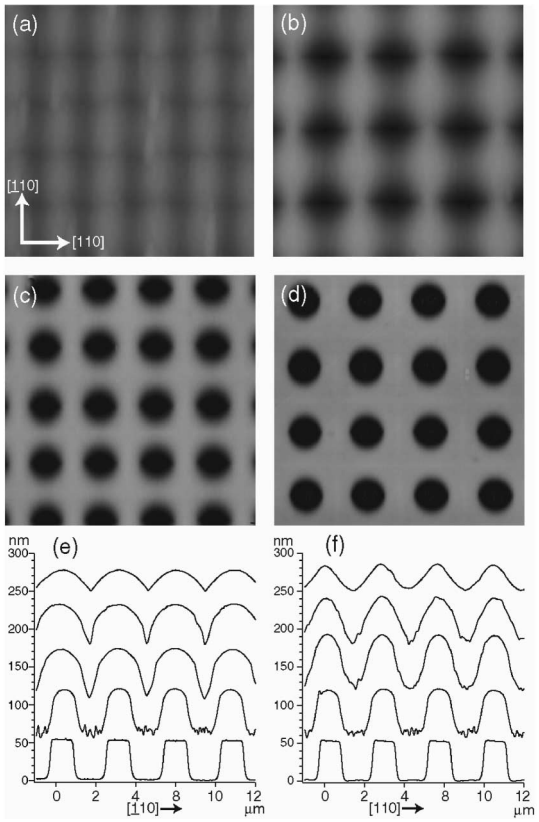

FIG. 1. (a)–(d) AFM images of the surface morphology after 500 nm thickness of growth of GaAs on the patterned GaAs(001) substrate patterned with a pit array of (a) 0.7 μm pit diameter and 1.4 μm center-to-center spacing, (b) 1.4 μm pit diameter and 2.8 μm spacing, (c) 2.8 μm pit diameter and 5.6 μm spacing, and (d) 5.6 μm pit diameter and 11.2 μm spacing. The overall gray scale of all the images is 75 nm. The sample orientation labeled in (a) is applied to all images shown in this Letter. (e),(f) Line profiles scanned, after growth, across the pit center from the same area where image in (b) was scanned. Those scanned along the [1$\bar{1}$0] direction are shown in (e) and the [110] direction in (f). In both panels, the bottom square wavelike profile is the initial surface. The thickness of the growth for the profile starting from the one next to the initial profile to the top is 100, 200, 300, and 500 nm, respectively.

For the largest diameter pits, the only visible change is a slight rounding of the edges without much change in the overall amplitude. The corrugations evolve faster along the [1$\bar{1}$0] direction than along the perpendicular [110] direction, resulting in visible eccentricity in the shape of the intermediate sized pits. Anisotropy in the evolution of GaAs(001) during growth is consistent with previous reports [7] and with the known anisotropy of the surface reconstruction of the surface [10,11]. Figures 1(e) and 1(f) show the evolution of line profiles across the pit centers along the [1$\bar{1}$0] and [110] directions, respectively. Profiles of the as-patterned surfaces are nearly square wave and isotropic. After 100 nm of growth, the sharp corners in the initial profile become rounded. Additional roughness in the form of "mounds" [6] appears at the bottom of the pits. The mounds, which initially grow but then disappear, are seemingly induced by the initial roughness associated with the reactive ion etching process used to pattern the surface. With further growth, the sidewalls of the pit close in along the [1$\bar{1}$0] direction, suppressing the further development of the mound associated roughness, and forming cusps at the center of each pit, which persist as growth continues. Line profiles along the [110] direction show an evolution to a near-sinusoidal shape.

Close inspection indicates that the overall amplitude of corrugation in the profiles shown in Figs. 1(e) and 1(f) first increases with growth, then decays. This is shown clearly in Fig. 2(a), which summarizes the evolution of the amplitude of the corrugation, normalized to its initial value, as a function the initial pit diameter. At each growth step, the length scale dependence of the amplitude shows nonmonotonic behavior, with a maximum corrugation at a diameter which shifts toward larger values as growth continues. This maximum marks the characteristic length scale at which the sense of the evolution changes. Beneath this diameter, further growth reduces the amplitude, while above it further growth amplifies the corrugation. This is qualitatively similar to what we have seen for AlAs/GaAs multilayer growth on patterned GaAs(001) [9].

There have been a number of continuum models [3–6] proposed to predict the evolution of surface roughness during growth; these might be expected to apply at the length scales of our patterned structures. Below we compare our experimental results with the predictions from four models that have received considerable attention. The first is the Kardar-Parisi-Zhang (KPZ) model [3], in which an instability in a flat surface to cusp formation results from fastest growth along the normal direction, and surface roughness smoothes out through evaporation and recondensation of atoms on the surface. The second model is that proposed by Sun *et al.* [5], which mathematically generalized the nonmass conserving KPZ equation into a conserved form (CKPZ). The third model we examine is the equation proposed by Lai and Das Sarma [4] for surface evolution under MBE growth.

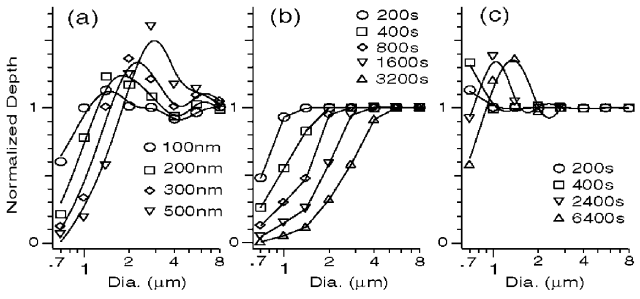

FIG. 2. The overall amplitude of the pit array corrugation measured after each growth from line profiles across the pit center along the [1$\bar{1}$0] direction normalized with its initial values, plotted as a function of the initial pit diameter for (a) experiment, (b) KPZ model, and (c) conserved KPZ model.

The last model was proposed by Johnson *et al.* [6], which attempted to explain their observation of mound formation during homoepitaxial growth on nominally flat GaAs(001) surfaces as due to the Ehrlich-Schwoebel effect [12,13]. As we show below, these four models predict distinctly different behavior, which we compare with our experimental results.

To compare the predictions of these models with our measurements, we start with the measured topography of as-patterned surfaces and use this to set the initial conditions for our numerical simulations, integrating the continuum equations using the finite difference method [14] to simulate the growth. Anisotropy between [110] and [1̄10] is introduced through an anisotropic version of the continuum equations [3–6], replacing the standard smoothing term in the height evolution equation $\upsilon\nabla^2 h$ with $\upsilon_x(\partial^2 h/\partial x^2) + \upsilon_y(\partial^2 h/\partial y^2)$ and the nonlinear, growth-related term $\lambda(\nabla h)^2$ with $\lambda_x(\partial h/\partial x)^2 + \lambda_y(\partial h/\partial y)^2$. We choose the x and y axes to correspond to the [110] direction and the [1̄10] direction, respectively; $h(x, y)$ describes the surface corrugation. A limitation of a number of the existing continuum equations proposed for growth is their phenomenological nature, i.e., the lack of a direct connection to physically based microscopic models. This makes it difficult to test the predictions of these equations using physically reasonable estimates of the values of the υ's and λ's; because of this, here we treat them as fitting parameters in our simulation. We find that ratios of υ_y/υ_x and λ_y/λ_x equal to 5 and 10, respectively, produce anisotropy similar to what was observed in the AFM images. The relative magnitudes between the υ's and the λ's are chosen within the range such that the growth terms play a significant role in the evolution. Our measurements indicate that the dominant features in the topography remain those at the pattern length scale over the range of growth we have explored; this implies that local fluctuations due to instantaneous and local variations in the flux are not significant for understanding our results. We therefore numerically integrated the equations with a negligible noise term.

Figure 3 shows the results of the simulations for a region on which the initial pit diameter was 0.7 μm, and the spacing is 1.4 μm, for each of the four models. Figures 3(a)–3(d) show grayscale representations of the surface morphology after allowing the simulations to run until a significant change in the morphology was visible. Figures 3(e)–3(h) show the evolution of line profiles across the pit centers along the [1̄10] direction. These make clear the major differences between the evolution predicted by the models. Figure 3(a) is for the KPZ model and shows the surface morphology after 1600 s of simulated growth. At this stage, the corrugations are partially smeared out along the [1̄10] direction, similar to what is seen in Fig. 1(a). The profiles in Fig. 3(e) show that the simulated growth very quickly produces cusps at the bottom of each pit center, which again is in qualitative

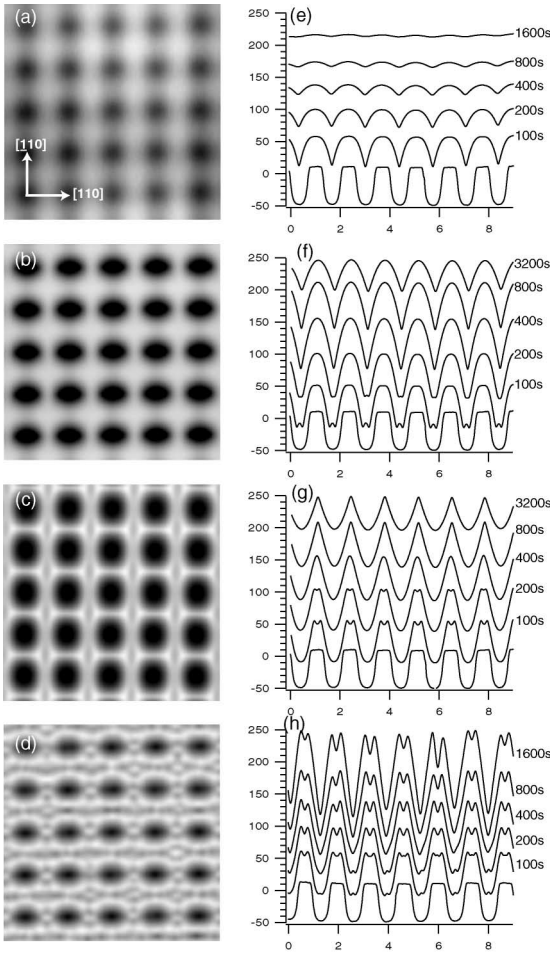

FIG. 3. (a)–(d) Numerically simulated surface morphology of the 0.7 μm diameter pit array and (e)–(h) the line profiles scanned along the [1̄10] direction. (a),(e) The KPZ model, with $\nu_x = 10$ nm^2/s and $\lambda_x = 1$ nm/s. (b),(f) The conserved KPZ model, with $\nu_x = 10^4$ nm^4/s and $\lambda_x = 10^3$ nm^3/s. (c),(g) The MBE model, with $\nu_x = 10^4$ nm^4/s and $\lambda_x = 10^3$ nm^3/s. (d),(h) The model by Johnson *et al.*, with $\nu_x = 10^4$ nm^4/s and $\lambda_x = 10$ nm^2/s. The equation for this model is $\partial h/\partial t = -\nabla^2(\nu_x\partial^2 h/\partial x^2 + \nu_y\partial^2 h/\partial y^2) - \nabla((\lambda_x\partial h/\partial x, \lambda_y\partial h/\partial y)/\{1 + a[\lambda_x(\partial h/\partial x)^2 + \lambda_y(\partial h/\partial y)^2]\})$, where $a = 100.0/\sqrt{\lambda_x\lambda_y}$.

agreement with the observed trend shown in Fig. 1(e). However, no initial amplification in corrugation is evident, in contrast to our observations. Figure 3(b) shows corresponding results for the CKPZ model after 3200 s of evolution. The most noticeable effect in this case is that each pit evolves from circular to elliptical in shape. The buildup of ridges of material between pits along the [1̄10] is not as pronounced in this case as for the KPZ model. Simulated growth line profiles for this model are shown in Fig. 3(f) and indicate trench formation around the bottom edges of the pits initially, which coalesce to single cusps at the bottom of each pit as growth proceeds. Significantly, the amplitude of the corrugations behaves nonmonotonically in time, with an initial amplification of the patterned corrugation. For both the KPZ and CKPZ model, the line profiles through the pit center along the

[110] direction (not shown) evolve into sinusoidal modulation, similar to those shown in Fig. 1(f). Figure 3(c) shows a grayscale image of the surface using the MBE equation to simulate 3200 s of growth. The general appearance is quite different from the AFM images shown in Fig. 1. Initially, a ring-shaped protrusion forms around each pit. Eventually, neighboring rings merge, forming persistent features, which are cusped direction but linear at right angles to this. The formation of cusps at the shoulders between neighboring pits is the opposite of what happens during growth, allowing us to exclude this model. Figure 3(d) shows the simulation according to the model proposed by Johnson *et al.* after 1600 s of simulated growth. This model predicts the formation of anisotropic mounds around and between the pits along the [$\underline{1}$10] direction. The evolution of the pits is anisotropic, as is seen in the experiment. However, both the grayscale image and the line profiles shown in Fig. 3(h) are distinctly different from what we observe in Fig. 1. The mounds join to the sidewalls of the pits, forming quasi-continuous rings about them. The sidewalls are nearly linear, and the angles that they make with respect to (001), as well as the overall corrugation, continue to grow monotonically with time. We thus exclude this model as well.

Of the four models that we have examined, only the KPZ and the conserved KPZ models predict morphological evolution that is qualitatively consistent with our observations during epitaxial growth. We thus restrict a more complete analysis of the predicted length scale dependence to these two models. Figures 2(b) and 2(c) show the simulated evolution of the corrugation vs initial pit diameter for the KPZ and CKPZ models, respectively. The results differ qualitatively from one another. The KPZ equation predicts a monotonic variation of the corrugation amplitude with lateral period and a monotonic decay with growth for any given initial pit diameter. This is inconsistent with the experimental results shown in Fig. 2(a). However, the CKPZ model [Fig. 2(c)] shows a peak in the corrugation with respect to lateral length scale, which moves to larger diameters with increased growth. The amplitude of the corrugation also behaves nonmonotonically with growth for a fixed initial diameter, with an initial amplification and an eventual decay, qualitatively consistent with our observations. The CKPZ model is thus in closest agreement with our patterned growth experiments. However, there are discrepancies. Most notably as seen in Fig. 2(a), our observations show a maximum corrugation amplitude which increases with growth, while those predicted by CKPZ are approximately constant.

This lack of complete agreement is not surprising. Since continuum models such as CKPZ were developed for describing the long term behavior of the surface roughness, only those terms which dominate in the asymptotic limit were kept in the height equation. In our case, the transient evolution of a surface that is artificially patterned with sharp edges would presumably require additional terms to be maintained. A modification of this and other continuum models to do so is beyond the scope of this Letter. Nevertheless, the comparison between the experiment and the simulation presented here demonstrates a straightforward approach for testing existing models in the technologically relevant transient regime and potentially could also provide guidance for further refinement of existing models.

Our observations of the evolution of the morphology of a patterned GaAs(001) surface shows the response of surface roughness to be nonmonotonic, with an initial amplification followed by decay and a characteristic lateral length scale, which divides these behaviors and whose value increases with further growth. These observations allow us to rule out the KPZ model for MBE growth in this system, in contrast to the conclusions of Ref. [8]. We find instead that, among the models proposed in the literature, the conserved KPZ model most closely reproduces what we observe. A corresponding atomic scale model based upon physical processes is needed to judge if this agreement is more than coincidental.

The authors acknowledge the technical assistance of L. Calhoun in the MBE growth of these samples, K. Limpaphayom in fabricating the samples, and R. Ankam for analyzing the results of the numerical simulations. This work was supported by the Laboratory for Physical Sciences and by NSF-MRSEC Grant No. DMR-0080008.

[1] A.-L. Barabasi and H. E. Stanley, *Fractal Concepts in Surface Growth* (Cambridge University, Cambridge, 1995).
[2] J. Villain, J. Phys. I (France) **1**, 19 (1991).
[3] M. Kardar, G. Parisi, and Y.-C. Zhang, Phys. Rev. Lett. **56**, 889 (1986).
[4] Z.-W. Lai and S. D. Sarma, Phys. Rev. Lett. **66**, 2348 (1991).
[5] T. Sun, H. Guo, and M. Grant, Phys. Rev. A **40**, 6763 (1989).
[6] M. D. Johnson *et al.*, Phys. Rev. Lett. **72**, 116 (1994).
[7] A. Ballestad *et al.*, Phys. Rev. B **65**, 205302 (2002).
[8] A. Ballestad *et al.*, Phys. Rev. Lett. **86**, 2377 (2001).
[9] S. Shah *et al.*, Appl. Phys. Lett. (to be published).
[10] V. P. LaBella *et al.*, Phys. Rev. Lett. **83**, 2989 (1999).
[11] M. Itoh *et al.*, Phys. Rev. Lett. **81**, 633 (1998).
[12] R. L. Schwoebel and E. J. Shipsey, J. Appl. Phys. **37**, 3682 (1966).
[13] G. Ehrlich and F. G. Hudda, J. Chem. Phys. **44**, 1039 (1966).
[14] T. J. Newman and A. J. Bray, J. Phys. A **29**, 7917 (1996).